

Supplementary Materials

Engineering a thermostability-enhanced active *Clostridium thermocellum* cellobiose phosphorylase by a combination of rational design and directed evolution

Xinhao Ye, Chenming Zhang, Y.-H. Percival Zhang

I. Primers

Table 1. Primers used in this study

Name	Sequence
<i>For plasmid construction</i>	
P1	5' GAAAGGCTGCAGCATGAAGTTCGGTTTTTTTG 3'
P2	5' CCTTTGGATCCTTATCCCATAATTAATTCAAC 3'
P3	5' AAAGTCTCGAGGGCTCTCCATGAAGTTCGGTTTTTTTG 3'
<i>For rational design</i>	
P1_130/131	5' GTGAAGTCCATTATCTTATATTGAAGAATGAAG 3'
P2_130/131	5' CATTGTAGTTTAACGGAACGAAGAAAG 3'
P1_201	5' AAATGCACCGATCAGCGGATTTG 3'
P2_201	5' ACAGAATAGAATGCGTAATGGTTTCTGC 3'
P1_292	5' GATAGAGCAGTTCAAGACTGTTG 3'
P2_292	5' ATTCATAAGCTTTTTCTTGTTGATG 3'
P1_411	5' AATGAAATCGGAGGCAACTTCAAC 3'
P2_411	5' GTTACCTTTTTGGTAAGAGGCTGATAC 3'
P1_423	5' GCTGATTCTTAGCCTGCTGCATATATTAAG 3'
P2_423	5' CACAACGGGTCATCGTTGAAGTTG 3'
P1_781	5' GTATCAAAGGTGTGAAAAAATAACTGTTGAC 3'
P2_781	5' ATGGTTCGGATTCTTACAGTGATTC 3'
<i>For directed evolution</i>	
P4	5' CGCCCAATACGCAAACC 3'
P5	5' CGCCATTCGCCATTCAGG 3'
P1_48	5' GGATATTGCTTTTACAAGGATGCAAGG 3'
P1_rs_48*	5' GGATATTGCTTTTACAGGGATGCAAGG 3'
P2_48	5' GCCTGCGGTATTCGAAATGAGTGAG 3'
P1_142	5' GGACAGGACAAAAAGAAAATAACTC 3'
P1_rs_142*	5' GGACAGGACAAAAAGAAAATAACTC 3'
P2_142	5' TTCATTCTTCAATATAAGCTTTGGACTTC 3'
P1_189	5' ACAGAGTACAGAGAGCTCAGAAACC 3'
P1_rs_189*	5' ACAGAGTACAGAGAGCGCAGAAACC 3'
P2_189	5' CTTGTGATAGATAACCGAGCCTTCAATC 3'
P1_526	5' CGGAAAAGACTATGCGAAGCTTTGC 3'
P1_rs_526*	5' CGGAAAAGACTATGTAAGCTTTGC 3'
P2_526	5' ATGAACACAAACATTCGGCAATCATAAC 3'

*primers used for reverse mutation



Fig. 1. Alignment of the CBP homology set, where IaCBP is from *Ignisphaera aggregans* (optimal growth temperature: 95 °C), TnCBP is from *Thermotoga neapolitana* (optimal growth temperature: 90 °C), TmCBP is from *Thermotoga maritime* (optimal growth temperature: 80 °C), DtCBP is from *Dictyoglomus thermophilum* (optimal growth temperature: 78 °C), CsaCBP is from *Caldicellulosiruptor saccharolyticus* (optimal growth temperature: 70 °C), CstCBP is from *Clostridium sterocorarium* (optimal growth temperature: 65 °C), CuCBP is from *Cellulomonas uda* (optimal growth temperature: 50 °C), BfCBP is from *Butyrivibrio fibrisolvens* (optimal growth temperature: 37 °C), and CgCBP is from *Cellvibrio gilvus* (optimal growth temperature: 30 °C). The candidates for substitution were selected based on the structural knowledge and highlighted with red frames. Ruler was designed in correspondence to the residue number of the first CBP sequence, IaCBP.

III. Stabilization centers

Stabilization center refers the residues that involved in cooperative long-range contacts, and are expected to stabilize proteins structures by preventing their decay with their cooperative long range interactions (Dosztányi et al. 1997). The stabilization centers of CtCBP were determined by SCider (<http://www.enzim.hu/scide>), in response to its homology modeling (Dosztányi et al. 2003).

Table 2. Stabilization centers of CtCBP

Resid. No.	Resid. Name	List of stabilization Centers	Resid. No.	Resid. Name	List of stabilization Centers	Resid. No.	Resid. Name	List of stabilization Centers
3	PHE	16	234	VAL	207, 208	622	LEU	648
4	GLY	14,15	239	ALA	208	623	GLN	647
12	GLU	99	241	ILE	150	624	ASN	582, 583
13	TYR	98	242	ALA	150	625	PRO	581
14	VAL	4, 97, 98	244	HIS	147, 204	635	GLY	486
15	ILE	4, 96	245	SER	146, 202, 203, 204	643	GLY	705
16	THR	3	253	GLY	135	647	ASN	623
22	TYR	691	254	GLU	135	648	ALA	622
41	ALA	69, 70	259	VAL	130, 131, 198	649	GLY	700, 701
42	GLY	68, 69, 70	260	PHE	129, 130, 197	650	ILE	700, 701
43	GLY	68, 69	261	ILE	128, 129, 196	651	PHE	700
45	CYS	55	264	TYR	193, 194	659	ILE	724
49	ASP	400	265	VAL	193	661	ALA	592
52	LEU	156	315	TYR	329, 758	691	LYS	22
54	ARG	155	316	PHE	757	696	VAL	715, 716
55	ILE	45, 153	317	LEU	756	697	TYR	715, 716, 718
56	THR	152, 153	329	ASN	315	698	ALA	714, 715, 716, 718, 720
57	ARG	152	332	ASN	725	699	GLN	713, 714
68	GLY	42, 43	335	GLN	718	700	MET	649, 650, 651
69	GLY	41, 42, 43	337	MET	372	701	VAL	649, 650
70	ARG	41, 42	338	VAL	717	705	ASP	643
73	TYR	146	343	SER	361	713	LYS	699
74	ILE	145, 146	356	GLY	398	714	ASN	698, 699
82	SER	92	357	MET	398	715	SER	696, 697, 698
92	LEU	82	361	ASP	343	716	TRP	696, 697, 698
93	GLU	109	363	ASN	381	717	LEU	338
96	GLU	15, 106	367	LEU	723	718	THR	335, 697, 698
97	CYS	14	372	GLN	337	720	THR	698
98	ARG	13, 14	381	LEU	363	723	TRP	367
99	HIS	12	388	GLN	443, 444	724	ASN	659
104	THR	118	396	HIS	406	725	PHE	332
105	LYS	118	398	TYR	356, 357	733	LEU	748
106	ILE	96	400	PRO	49	741	GLY	795
109	LYS	93	406	ASN	396	742	LEU	794
113	ILE	135, 136	420	LEU	460	743	LYS	794
114	LYS	134	421	ILE	457	748	ILE	733, 776
118	THR	104, 105	439	GLU	452	750	LYS	775, 776
119	PHE	129	440	GLN	451, 452	752	TRP	772, 775
128	GLU	261	441	VAL	451, 453	753	ASP	772
129	VAL	119, 260, 261	443	PHE	388	756	LYS	317
130^a	GLN	259, 260	444	ASN	388	757	VAL	316, 767
131^a	LYS	259	451	ASP	440, 441	758	THR	315
134	LEU	114	452	THR	439, 440	763	GLY	800
135	LYS	113, 253, 254	453	MET	441	765	THR	802, 803
136	ASN	113	457	LEU	421	766	TYR	804
145	THR	74	460	SER	420	767	GLU	757
146	LEU	73, 74, 245	472	GLY	551	769	THR	807
147	PHE	244	474	PRO	510, 511, 514	770	VAL	808
150	ILE	241, 242	475	LEU	510, 514	771	LYS	809
152	PHE	56, 57	476	ILE	510, 511, 514	772	ASN	752, 753
153	CYS	55, 56	486	ASN	634, 635	775	HIS	750, 752
155	TRP	54	510	GLU	474, 475, 476	776	VAL	748, 750, 810
156	ASN	52	511	SER	474, 476	779	GLY	810

179	VAL	196	514	ILE	474, 475, 476	780	VAL	810
193	TYR	264, 265	518	PHE	548	781^b	ALA	809, 810
194	ALA	264	548	MET	518	782	LYS	808
196	TYR	179, 261	551	ALA	472	783	ILE	807
197	SER	260	560	GLU	605, 606	794	ILE	742, 743
198	VAL	259	561	TRP	574, 575	795	LEU	741
202	ILE	245	563	LEU	574	800	ASP	763
203	SER	245	574	GLY	563, 563	802	LYS	765
205	PHE	231, 232	575	SER	561	803	THR	765
206	ASP	231, 232, 233	581	GLY	625	804	HIS	766
207	SER	233, 234	582	LYS	624	807	GLU	769, 783
208	ASP	235, 234, 239	583	ILE	624	808	VAL	770, 782
231	ASN	205, 206	592	VAL	661	809	ILE	771, 781
232	ASN	205, 206	605	LYS	560	810	MET	776, 779, 780, 781
233	SER	206, 207, 208	606	ALA	560			

^a The residues Q130 and K131 were located in the stabilization centers in pair, both interacting with V259 and/or Y258. Mutation Q130H and K131Y generated strong π - π interactions and expanded the stabilization centers of both resid 130 and 131 to F119 and F260. Therefore, they were chosen for site-directed mutagenesis, resulted in a 1.7-fold increase of the inactivation half-time at 70 °C.

^b The residues A781 was located in the stabilization centers. The substitution of A781 with Lysine didn't change its own stabilization center partners, whereas increased the stabilizing partners of T765 with T803, Y766 with P796, and V767 with H804. Therefore, the mutation A781K expanded the stabilization centers and, practically, increased the inactivation half-time to 15.3 min.

IV. Protein contact map

A protein contact map represents the distance between all possible residue pairs of a 3-D protein structure. The contact map of *CtCBP* was established by Contact Map plugin of VMD 1.8.6 (Humphrey et al. 1996).

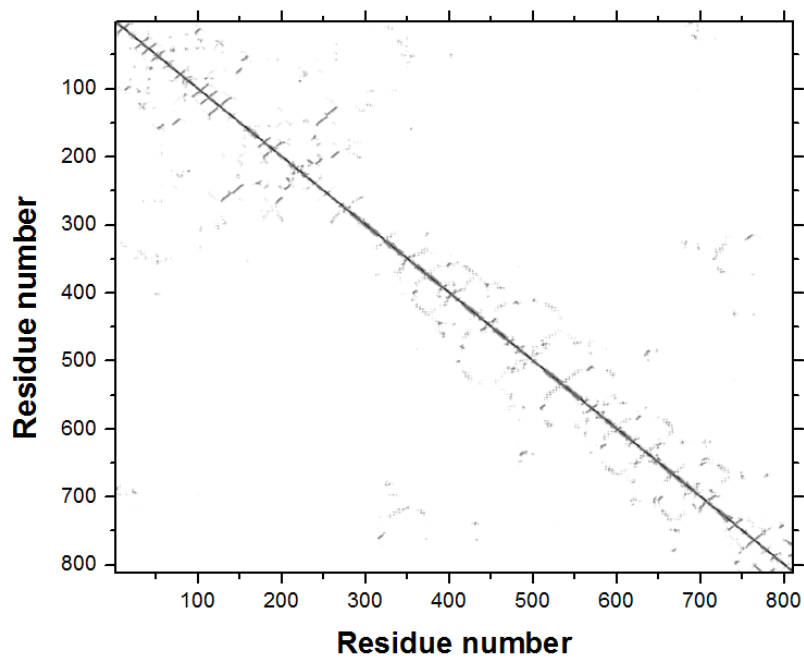


Fig.2 Contact map of *CtCBP*. A graph square is colored black at 0.0 Angstrom distance, to a linear gray scale between 0.0 and 10.0 Angstroms, and white when equal to or greater than 10.0 Angstroms.

V. Optimal mutation rate for the random mutagenesis of CtCBP

Given a choice of protein scaffold, libraries of fixed sizes, and no reliable knowledge for rational engineering, a simple assessment of library optimality is the number of valuable clones they contain (Daugherty et al. 2000). Therefore, it is hard to tell if we have reasonable mutation rates before qualitative and quantitative evaluation of both low- and high- frequency mutagenesis libraries.

Although the optimal conditions for making mutant libraries are unclear, it is well believed an optimal mutation rate exists that balances diversity and retention of the function (Miura and Sonigo 2001; Zacco and Gherardi 1999). In general, low-error-rate mutagenesis results in a high probability of functional sequences with a low probability of beneficial mutations, while high-error-rate mutagenesis brings out a high probability of lethal mutations with a high probability of unique sequences. In the past decades, there have been many attempts to determine the optimum mutation rates for directed evolution theoretically and experimentally (Clune et al. 2008; Kimura 1960; Pritchard et al. 2005; Shafikhani et al. 1997; Zacco et al. 1996). Daugherty *et al.* quantitatively analyzed the effect of mutation frequency on the affinity maturation of single chain Fv antibodies (2000). At the low to moderate mutation frequencies with an average mutation rate of $m \leq 8$, the functional fraction of clones decreased exponentially, but the most highly mutated library ($m = 22.5$) had significantly more active clones than expected relative to this trend. The results indicated a preferred mutation frequency for functional improvement of scFv may persist between $m = 4$ and $m = 2$, under which the library includes a larger fraction of active mutants and is more likely to yield improved mutants. Miura and Sonigo proposed a simple model to determine the optimal mutation rate for random mutagenesis (2001). They linked the optimal rate with the number of simultaneous mutations required for possible beneficial and lethal changes. As a result, the model predicted the optimum is a mutation rate that induces at least 63% ($1 - e^{-n}$, n represents the required number of positive mutations and $n \geq 1$) of the cloned gene in the library to be non-functional.

Recently, a more inclusive model was presented by Drummond *et al.* (2005a). In their work, experimental data firstly proved that the mutations do not follow the Poisson distribution under the high-error-rate random mutagenesis, but rather a previously proposed distribution derived from a PCR model (Sun 1995). The PCR-distributed mutations were then modeled to investigate the effect of mutation rates on functionally improved fractions in the random mutagenesis libraries. It was found that the optimal mutation rates depend on the number of transformants sampled, the PCR protocol used, the wild-type protein being mutated, and other parameters. Considering it's the most realistic model of error-prone PCR by far, we followed Sun's and Drummond's model to estimate the possible optimum in our work as below.

Assume the *cbp* gene would be amplified by error-prone PCR with a constant efficiency λ . Here λ is set as 0.6 (Drummond et al. 2005a). The thermal cycles are n , resulting in $d = n\lambda$ DNA doublings. Based on Sun's model (Sun 1995), the average of nucleotide mutations per sequence, say $E(m_n)$, is defined as

$$E(m_n) = \frac{n\lambda\mu G}{1 + \lambda} \quad (1)$$

where μ and G represent mutation rate (mutations per base per PCR cycle) and gene length, respectively. Set

$$x = \mu G \quad (2)$$

which actually presents another type of mutation rate (mutations per PCR cycle).

Then the mutational distribution can be computed as follows,

$$\begin{aligned} P(M = m_{nt}) &= \sum_{k=0}^n P(M = m|K = k)P(K = k) \\ &= \sum_{k=0}^n \frac{(kx)^{m_{nt}} e^{-kx}}{m_{nt}!} \frac{\binom{n}{k} \lambda^k}{(1 + \lambda)^n} = \frac{x^{m_{nt}}}{(1 + \lambda)^n m_{nt}!} \sum_{k=0}^n \binom{n}{k} \lambda^k k^{m_{nt}} e^{-kx} \end{aligned} \quad (3)$$

The probability a nucleotide mutation produces a non-synonymous change is assumed to be binomial, with parameter p_{ns} . Generally, p_{ns} is around 0.8 (Daugherty et al. 2000). Note that non-synonymous variations include the changes of amino acid encoded as well as the others that truncated or inactivated the protein (e.g. insertions, deletions, and mutations to stop codons). The latter constitutes a fraction of mutation with the probability p_{tr} . The p_{tr} is around 0.05-0.07 (Drummond et al. 2005b) and assumed to be 0.06 here. Then the probability a sequence with m_{nt} nucleotide mutations retains function can be defined as

$$\begin{aligned} P(f | m_{nt}) &= \sum_{m_{ns}=0}^{m_{nt}} \binom{m_{nt}}{m_{ns}} P(\text{non trunc.} | m_{ns}) \times P(f | m_{ns} \text{ amino acid changes}) \\ &= (1 - (1 - v(1 - p_{tr}/p_{ns}))p_{ns})^{m_{nt}} \end{aligned} \quad (4)$$

where m_{ns} denotes non-synonymous mutation, and v represents the average fraction of functional one-mutant neighbors on the protein-sequence-space network. By combining eq.(3) and (4), and assuming gene length $L \rightarrow \infty$ since $\langle m_n \rangle \ll L$, we find the probability a sequence from the library will retain function is:

$$P(f) = \sum_{m_{nt}=0}^{\infty} P(f | m_{nt})P(m_{nt}) = \left(\frac{1 + \lambda \left(-\frac{\langle m_{nt} \rangle (1 + \lambda)}{n\lambda} (1 - v(1 - p_{tr}/p_{ns}))p_{ns} \right)}{1 + \lambda} \right)^n \quad (5)$$

Now v is required to predict the functional fractions. In this work, since the surviving colonies in selection plates represent the functional mutants, the probability $P(f)$ would approximate the selection power of each library. Using the $\langle m_{nt} \rangle$ vs. selection power data, we then estimate the random mutagenesis of *Ctcbp* with $v \approx 0.91$ (see SOM-Fig. 3). Intriguingly, the v value is much bigger than previous reports ($v \approx 0.2$ for the antibody binding task, and $v \approx 0.65$ for the subtilisin data), thanks to the larger sequence of *Ctcbp*. It

suggests a low probability to inactivate CtCBP by one-mutant-per-step spacewalk, which is helpful to produce functional mutants, but limits the unique fractions.

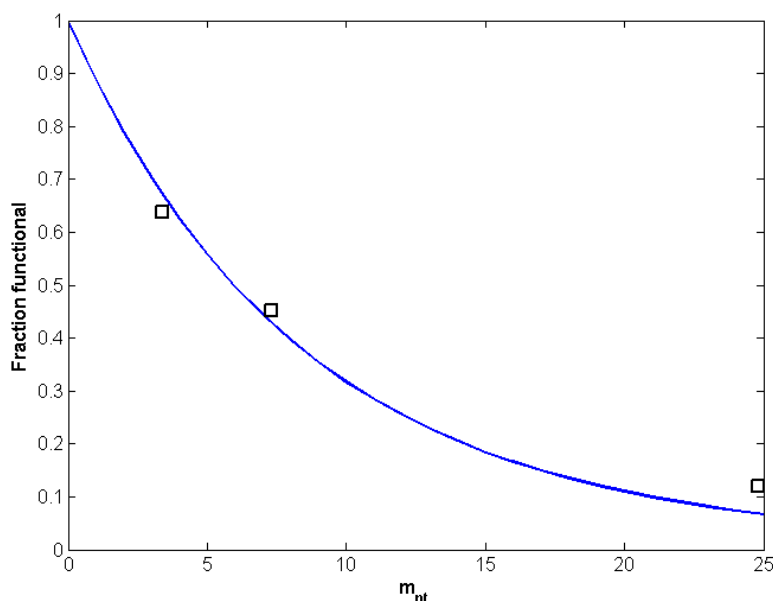


Fig. 3 Regression analysis of the experimental data (m_{nt} vs. selection power) to estimate v . The blue line fits the data ('□') in Matlab 2009a (MathWorks, Natick, MA), based on the equation (5).

Next, the probability that a non-truncated sequences with m_{nt} substitutions can be calculated by

$$P(\text{non-truncated} | M = m_{nt}) = (1 - p_{tr} / p_{ns})^{m_{nt}} \quad (6)$$

Suppose there are N transformants in the epPCR library. On average,

$$N_m = N \cdot P(M = m_{nt}) P(\text{non-truncated} | M = m_{nt})$$

are non-truncated proteins with m nucleotide mutations.

If with one nucleotide mutation per codon, an average of 5.7 amino acid substitutions (out of a maximum of 19) is accessible due to the conservatism of the genetic code, the m nucleotide mutations will conduce to

$$M_m = \binom{L/3}{m} 5.7^m \quad (7)$$

the average number of unique proteins, where L is the length of the gene in nucleotides.

Give N_m samples, the expected number of unique sequences produced by equal-probably sampling M_m sequences is

$$U_m = M_m - M_m(1 - 1/M_m)^{N_m} \approx M_m(1 - e^{-N_m/M_m}) \quad (8)$$

Consequently, the total number of unique sequences in a library is the sum over all unique sequences with a specific number of substitutions:

$$U = \sum_{m=0}^{L/3} U_m \quad (9)$$

and the number of unique sequences that retain at least wide-type function is

$$U_f = \sum_{m=0}^{L/3} U_m v^m \quad (10)$$

Finally, the fraction of unique sequences ($P(U)$) and unique functional sequences ($P(U_f)$) are

$$P(U) = U/N \quad (11)$$

$$P(U_f) = U_f/N \quad (12)$$

respectively. The relationship between mutation rates and fraction unique sequences is shown in SOM-Fig. 4. It is clear the unique sequences are enriched in the high-frequency mutagenesis. However, the maximum fraction of unique sequences is relatively small ($P(U) < 0.5$) even as $\langle m_{nt} \rangle = 6$, because sequences truncated by frameshifts and stop codons accumulate at increasing levels as the mutation rate is increased (Drummond et al. 2005a; Miura and Sonigo 2001).

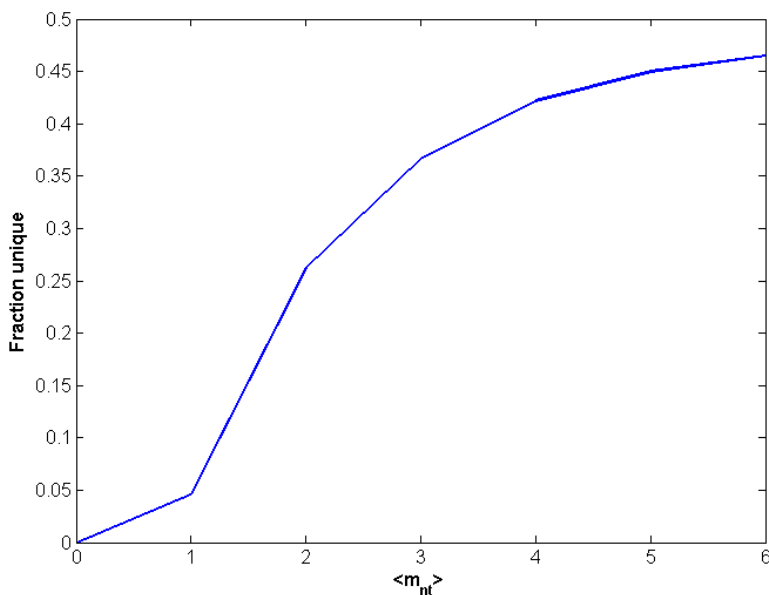


Fig. 4 The relationship between error rates and fraction of unique sequences. The line is simulated by eq. (11) with $n = 25$ thermal cycles, efficiency $\lambda = 0.6$, and library size $N = 10,000$ clones.

SOM-Fig. 5 illustrates the effects of mutation rates on the fraction of unique functional sequences $P(U_f)$. The results suggest optimal mutation rates are both protocol and protein-dependent. Under current circumstances with $n = 25$ thermal cycle, Taq DNA polymerase ($\lambda = 0.6$) and the structural plasticity ($\nu = 0.91$, $p_{ns} = 0.8$, $p_{tr} = 0.07$), we predict the optimal mutation rate for random mutagenesis of *Ctcbp* is 6 mutations per gene (SOM-Fig.4), which theoretically yield 4500+ unique mutants and more than 3,000 unique & functional CBP mutants over the 10,000 clones.

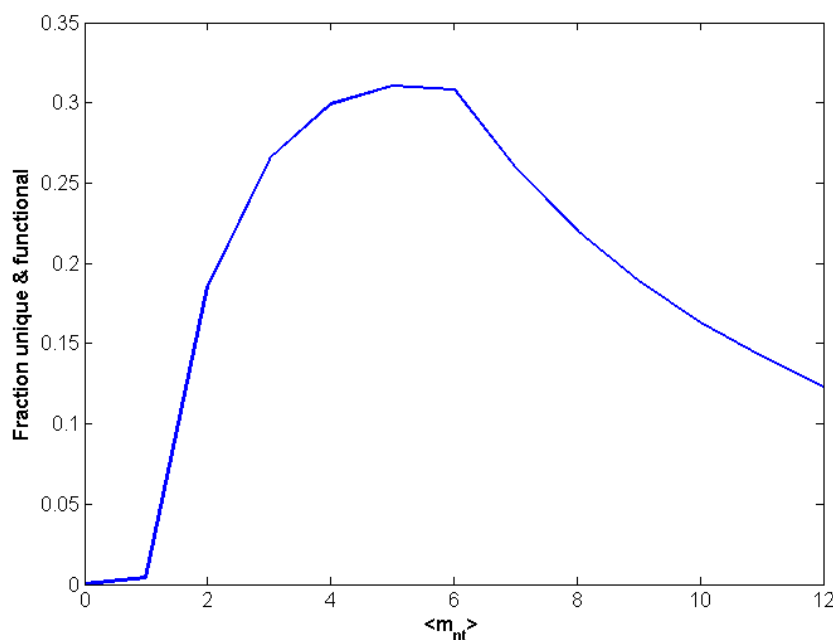


Fig. 5 The effect of mutagenesis frequencies on fraction of unique and functional sequences. The blue line is estimated by eq. (12) with $n = 25$ thermal cycles, PCR efficiency $\lambda = 0.6$, $p_{ns} = 0.8$, $p_{tr} = 0.07$, and library size $N = 10,000$ clones.

Based on previous work in our lab (Liu et al. 2009), we can achieve such a mutation rate ($\sim 0.25\%$) under the condition with regular PCR buffer with 5 mM $MgCl_2$ plus 3 mM $MnCl_2$, 0.2 mM dATP, 0.2 mM dGTP, 1 mM dCTP, and 1 mM dTTP. Practically, it resulted to a mutant library (Library O) with an average mutation rate 0.28%.

References:

- Bloom JD, Silberg JJ, Wilke CO, Drummond DA, Adami C, Arnold FH. 2005. Thermodynamic prediction of protein neutrality. *Proc Nat Acad Sci USA* 102(3):606-611.
- Clune J, Misevic D, Ofria C, Lenski RE, Elena SF, Sanjuán R. 2008. Natural Selection Fails to Optimize Mutation Rates for Long-Term Adaptation on Rugged Fitness Landscapes. *PLoS Comput Biol* 4(9):e1000187.
- Daugherty PS, Chen G, Iverson BL, Georgiou G. 2000. Quantitative analysis of the effect of the mutation frequency on the affinity maturation of single chain Fv antibodies. *Proc Nat Acad Sci USA* 97(5):2029-2034.
- Dosztányi Z, Fiser A, Simon I. 1997. Stabilization centers in proteins: Identification, characterization and predictions. *J. Mol. Biol.* 272(4):597-612.
- Dosztányi Z, Magyar C, Tusnády G, Simon I. 2003. SCide: identification of stabilization centers in proteins. *Bioinformatics* 19(7):899-900.
- Drummond DA, Iverson BL, Georgiou G, Arnold FH. 2005a. Why high-error-rate random mutagenesis libraries are enriched in functional and improved proteins. *J. Mol. Biol.* 350(4):806-816.
- Drummond DA, Silberg JJ, Meyer MM, Wilke CO, Arnold FH. 2005b. On the conservative nature of intragenic recombination. *Proc Nat Acad Sci USA* 102(15):5380-5385.
- Humphrey W, Dalke A, Schulten K. 1996. VMD: Visual molecular dynamics. *J. Mol. Graphics* 14(1):33-38.
- Kimura M. 1960. Optimum mutation rate and degree of dominance as determined by the principle of minimum genetic load. *J Genet* 57(1):21-34.
- Liu W, Hong J, Bevan DR, Zhang Y-HP. 2009. Fast identification of thermostable beta-glucosidase mutants on cellobiose by a novel combinatorial selection/screening approach. *Biotechnol. Bioeng.* 103(6):1087-1094.
- Miura T, Sonigo P. 2001. A mathematical model for experimental gene evolution. *J. Theor. Biol.* 209(4):497-502.
- Pritchard L, Corne D, Kell D, Rowland J, Winson M. 2005. A general model of error-prone PCR. *J. Theor. Biol.* 234(4):497-509.
- Shafikhani S, Siegel R, Ferrari E, Schellenberger V. 1997. Generation of large libraries of random mutants in *Bacillus subtilis* by PCR-based plasmid multimerization. *BioTechniques* 23(2):304-310.
- Sun F. 1995. The polymerase chain reaction and branching processes. *J. Comput. Biol.* 2(1):63-86.
- Zaccolo M, Gherardi E. 1999. The effect of high-frequency random mutagenesis on *in vitro* protein evolution: a study on TEM-1 β -lactamase. *J. Mol. Biol.* 285(2):775-783.
- Zaccolo M, Williams DM, Brown DM, Gherardi E. 1996. An Approach to Random Mutagenesis of DNA Using Mixtures of Triphosphate Derivatives of Nucleoside Analogues. *J. Mol. Biol.* 255(4):589-603.